Computer Modeling in Engineering & Sciences CMES, vol.122, no.3, pp.1099-1118, 2020

Integral Transform Method for a Porous Slider with Magnetic Field and Velocity Slip

Naeem Faraz[1,*], Yasir Khan[2], Amna Anjum[1] and Anwar Hussain[3]

Abstract: Current research is about the injection of a viscous fluid in the presence of a transverse uniform magnetic field to reduce the sliding drag. There is a slip-on both the slider and the ground in the two cases, for example, a long porous slider and a circular porous slider. By utilizing similarity transformation Navier-Stokes equations are converted into coupled equations which are tackled by Integral Transform Method. Solutions are obtained for different values of Reynolds numbers, velocity slip, and magnetic field. We found that surface slip and Reynolds number has a substantial influence on the lift and drag of long and circular sliders, whereas the magnetic effect is also noticeable.

Keywords: Porous slider, MHD flow, Reynolds number, velocity slip, integral transform method.

Nomenclature

β_1, β_2	Slip factors	μ	dynamic viscosity
τ	Extra stress tensor	$\mathbf{I}$	Identity tensor
p	pressure	d	width
x, y, z	Space coordinates	u, v, w	Velocity function
H_1, H_2	Slip coefficient	v_0	Constant viscosity
B_0	Magnetic field	ψ_1, ψ_2, ψ_3	Velocity Components
η	Similarity variable	ρ	Fluid Density
l	Length	d	width

[1] International Cultural Exchange School (ICES), Donghua University, Shanghai, China.

[2] Department of Mathematics, University of Hafr Al-Batin, Hafar Al-Batin, Saudi Arabia.

[3] DBS & HCEME, National University of Science and Technology, Islamabad, Pakistan.

[*] Corresponding Author: Naeem Faraz. Email: nfaraz_math@yahoo.com.

Received: 20 August 2019; Accepted: 09 October 2019.

1 Introduction

It is well-established fact that moving body reduces the drag if it is elevated by a layer of air. There are different examples such as air-cushioned vehicles and air hockey, which reduces the frictional resistance of moving objects. Skalak et al. [Skalak and Wang (1975)] were the pioneers to study a three-dimensional flow arising between moving the porous flat plate and the ground. In the case of Newtonian fluids, past researches include the circular, long and elliptical porous sliders. A large literature is available related to the Long Porous Slider (LPS) [Skalak and Wang (1975); Khan, Wu, Faraz et al. (2011); Awati and Jyoti (2016); Faraz, Khan, Lu et al. (2019); Sinha and Adamu (2017); Khan, Faraz, Yildirim et al. (2011)] and the Circular Porous Slider (CPS) [Faraz (2011); Wang (1974, 1978, 2012); Madani, Khan, Mahmodi et al. (2012)**;** Ghoreishi, Ismail and Rashid (2012)]. Naeem studied the influence of Reynolds number (R) on the CPS [Faraz (2011)] and the LPS [Faraz, Khan, Lu et al. (2019)]. Ghoreishi also studied the CPS [Ghoreishi, Ismail and Rashid (2012)]. Madani investigated a CPS by using Homotopy Perturbation Method (HPM) and also analyzed the lift and drag [Madani, Khan, Mahmodi et al. (2012)]. In a separate study, Khan also studied the effects of Reynolds number by using different analytical methods [Khan, Wu, Faraz et al. (2011); Khan, Faraz, Yildirim et al. (2011)]. Awati also investigated the lubrication of the LPS by using Homotopy Analysis Method (HAM) [Awati and Jyoti (2016)].

All the above-mentioned studies were done without slip condition on both the immobile ground and slider. Whenever the slip condition is particularly essential for super-hydrophobic planes. It became/is difficult to have zero mean tangential velocity from where the fluid is injected when there is a slip. Furthermore, in order to minimize adhesion, the fluid could be a rarefied gas, where compact exterior could be coated with a material or the ground could be uneven such that an equivalent slip exists or there is a slip flow regime. Wang [Wang (2012)] discussed the slip effects but didn't consider the effects of the transverse magnetic field [Turkyilmazoglu (2016, 2018, 2019a, 2019b)]. As the slow movement of a fluid may be characterized by streamlines, indicative of regular, orderly motion, called laminar flow. As the flow velocity is increased, or the space available made larger, there is a point where any small disturbance is amplified and the flow breaks up into turbulence. Then the velocity profile and all the other flow characteristics change radically. This is especially familiar in pipe flow, in the transition from laminar Poiseuille flow to turbulent flow. The criterion is the dimensionless Reynolds number, which indicates the relative importance of inertial and viscous forces. A magnetic field may be expected to stabilize a flow against the transition to turbulent flow. That is the reason why, cases of the magnetic field normal to the flow, have been studied, and the stabilizing effect observed. Experiments have been made that show this general result, but they are difficult and quantitatively not very conclusive. Similarly, another kind of instability occurs when there is a temperature gradient and a pressure gradient in the same direction, such as occurs in the lower atmosphere or in a pot of liquid heated on a stove. A magnetic field in the direction of the temperature and pressure gradient will hinder the transverse motion essential to convection, and make the convective "cells" narrower and less efficient, reducing the rate of energy transfer.

Therefore, the goal of the current work is to examine the impact of slip and Reynolds number when there is a transverse magnetic field on the performance of the porous slider. Literature survey clearly indicates that no solutions have been given for the three-dimensional flows of this type with slip and a uniform magnetic field. Hence, the goal of the current research is to analyze the performance of the porous slider in the presence of slip and Reynolds number with a constant magnetic field and to assess their effects on the components of velocity lift and drag.

Structure of the article is arranged as follows: In the introduction, we presented a brief history of the problem of the porous slider and its application. In second and third sections we discussed the formulation of the problem and the method to be used to solve the resulting problems of the long and the CPS. This paper adopted an Integral Transform Method (ITM) [Faraz, Khan, Lu et al. (2019)] that comprises both Variation Iteration Algorithm-II (VIM-II) and Adomian Decomposition Method (ADM) to reduce the computational work. VIM-II is the improved form of Variation Iteration Algorithm-I (VIM-I), proposed by Faraz in 2010 [Faraz, Khan and Austin (2010)]. Apparently, the final formulation of the proposed method has great symmetry with the existing methods such as VIM-I [El-Sayed and El-Mongy (2018); Wazwaz and Kaur (2019)] and ADM [Patel and Meher (2016); de Vargas Lisbôa and Marczak (2018); Turkyilmazoglu (2019c)] but this method does not need to calculate the Lagrange multiplier separately and gives a direct formulation of VIM-II, which avoids the unnecessary calculations, which is one of the goals of our study is to introduce a new method based on integral transformation to cover the shortcomings of the VIM-I, VIM-II, and ADM for solving nonlinear boundary value problems given in Eqs. (7), (8), (9), (12), (28), (29) and (32). The LPS solved by Khan et al. in 2011 [Khan, Wu, Faraz et al. (2011); Khan, Faraz, Yildirim et al. (2011)] involves unnecessary and repeated calculations. Similarly, section four five and six are related to problem formulation and solution of the long and the CPS respectively. Section seven is based on results and discussion and finally, the last part is the conclusion.

2 Problem formulation

As discussed above, in this study we will consider velocity slip condition. Navier introduced the slip condition for the first time as follows:

$$u = H\varsigma \tag{1}$$

In Eq. (1) tangential velocity u is proportional to the shear stress and tangential velocity are directly proportional to each other with H as the constant of proportionality which is actually a slip coefficient. In order to ignore the end effects, it is assumed that the gap between slider and ground is quite small as compared to the slider's lateral dimension. We tried to study both the CPS and LPS.

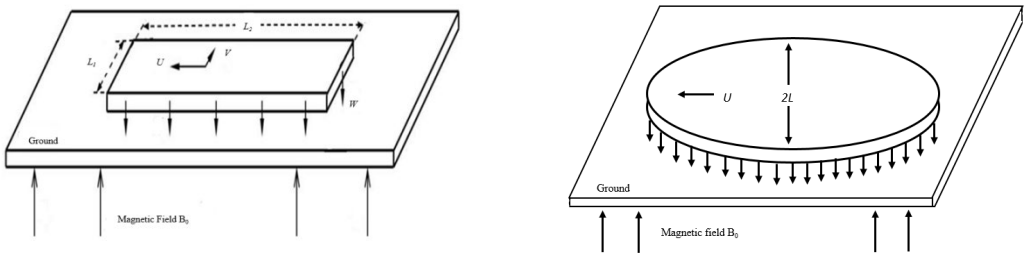

(a) (b)

Figure 1: (a): Schematic diagram of moving the long porous slider; (b): Schematic diagram of moving the long circular slider

We take the incompressible and steady flow of a viscous fluid between a porous (long and circular) slider and the ground in the presence of a uniform magnetic field as shown in Fig. 1. Length and width are quite big as compared to the width d. The slider moves with velocity components and elevated because of injection of fluid from its bottom with a magnetic field which is applied externally. In order to avoid the induced magnetic field formed by the movement of fluid, it is assumed that the magnetic Reynolds number is not very big. Furthermore, the induced and imposed electric field are supposed to be negligible, therefore the electromagnetic body force per unit volume simplifies $\mathrm{F}_{em}=\sigma_0\left(\mathrm{v}\times\mathrm{B}\right)\times\mathrm{B}$, where $\mathrm{B}=\left(0,0,B_0\right)$ is the magnetic field. Under the above-stated assumptions and conditions, Navier Stokes equations take the following form:

$$u\frac{\partial u}{\partial x}+v\frac{\partial u}{\partial y}+w\frac{\partial u}{\partial z}=-\frac{1}{\rho}\frac{\partial p}{\partial x}+\upsilon\left(\frac{\partial^2 u}{\partial x^2}+\frac{\partial^2 u}{\partial y^2}+\frac{\partial^2 u}{\partial z^2}\right)-\frac{\sigma_0}{\rho}B_0^2 u \tag{2}$$

$$u\frac{\partial v}{\partial x}+v\frac{\partial v}{\partial y}+w\frac{\partial v}{\partial z}=-\frac{1}{\rho}\frac{\partial p}{\partial y}+\upsilon\left(\frac{\partial^2 v}{\partial x^2}+\frac{\partial^2 v}{\partial y^2}+\frac{\partial^2 v}{\partial z^2}\right)-\frac{\sigma_0}{\rho}B_0^2 v \tag{3}$$

$$u\frac{\partial w}{\partial x}+v\frac{\partial w}{\partial y}+w\frac{\partial w}{\partial z}=-\frac{1}{\rho}\frac{\partial p}{\partial z}+\upsilon\left(\frac{\partial^2 w}{\partial x^2}+\frac{\partial^2 w}{\partial y^2}+\frac{\partial^2 w}{\partial z^2}\right)-\frac{\sigma_0}{\rho}B_0^2 w \tag{4}$$

where (u,v,w) are the velocity components in Cartesian coordinate $\left(x,y,z\right)$, where ρ, p and υ are density, pressure and kinematic viscosity respectively. Law of conservation of mass is as follows:

$$\frac{\partial u}{\partial x}+\frac{\partial v}{\partial y}+\frac{\partial w}{\partial z}=0 \tag{5}$$

The system of equations in a steady, compressible, laminar boundary layer is composed of two fundamental equations. Those are the continuity equation and the momentum equation. The solutions of these equations, when solved simultaneously for a two-dimensional boundary layer, are the velocity in the x, y and z direction $\left(u,v,w\right)$. The

system of equations is a system of partial differential equations (PDE) and is usually difficult to solve. Therefore, sophisticated transformation methods, called similarity transformations are introduced to convert the original partial differential equation set to a simplified ordinary differential equation (ODE) set. To do so we introduce the following similarity transformations [Faraz, Khan, Lu et al. (2019)].

$$u = U\psi_1(\eta) + \frac{W}{d} x\psi_3'(\eta), v = V\psi_2(\eta), w = -W\psi_3(\eta). \tag{6}$$

where $\eta = \frac{W}{d}$. By using Eq. (6) into Eqs. (2)-(4), we get the following ordinary differential equations

$$\psi_3^{iv} = R\left(\psi_3'\psi_3'' - \psi_3\psi_3'''\right) + M^2\psi_3' \tag{7}$$

$$\psi_1'' = R\left(\psi_1\psi_3' - \psi_3\psi_1'\right) + M^2\psi_1 \tag{8}$$

$$\psi_2'' = -R\left(\psi_1\psi_2'\right) + M^2\psi_2 \tag{9}$$

where R is the Reynolds number ($R = Wd/\upsilon$). Boundary conditions at $z = 0$ and $z = d$ are given in Eqs. (10) and (11) respectively.

$$u = U + H_1\mu\frac{\partial u}{\partial z}, v = V + H_1\mu\frac{\partial v}{\partial z}, w = 0 \tag{10}$$

$$u = -H_2\mu\frac{\partial u}{\partial z}, v = -H_2\mu\frac{\partial v}{\partial z} = 0, w = -W \tag{11}$$

Here H_1, H_2 and $\mu = \rho\upsilon$ are slip coefficients and viscosity respectively. Eqs. (10) and (11) gives

$$\begin{aligned}
&\psi_3'(0) = \beta_1\psi_3''(0) =, \psi_3(0) = 0,\\
&\psi_3(1) = 1, \psi_3'(1) = -\beta_2\psi_3''(1),\\
&\psi_1(1) = -\beta_2\psi_1'(1), \psi_1(0) - 1 = \beta_1\psi_1'(0),\\
&\psi_2(1) = -\beta_2\psi_2'(1), \psi_2(0) - 1 = \beta_1\psi_2'(0).
\end{aligned} \tag{12}$$

where $\beta_1 = H_1\mu/d, \beta_2 = H_2\mu/d$ are slip factors. Eqs. (7)-(9) and (12) will be solved by using ITM. We can deduce the expression for pressure from Eqs. (2)-(4) as follows:

$$-\frac{p}{\rho} = \frac{W^2\Lambda x^2}{2d} + \frac{1}{2}w^2 - \gamma\frac{\partial w}{\partial z} + A \tag{13}$$

where Λ, A are constants and

$$\Lambda = \left(\psi_3'\right)^2 - \psi_3\psi_3'' - \frac{1}{R}\psi_3''' = \left(\psi_3'(0)\right)^2 - \frac{1}{R}\psi_3'''(0). \tag{14}$$

If we take $2l$ as the width of the slider with ambient pressure ρ_0, then Eq. (13) gives

$$p - p_0 = -\rho \frac{\Lambda W^2 \left(x^2 - l^2\right)}{2d^2}. \tag{15}$$

The relationship between depth and lift can be expressed as follows:

$$L = \int_{-1}^{1} \left(p - p_0\right) dx = \frac{2\rho W^2 l^3}{3d^2} \Lambda. \tag{16}$$

where $2\rho W^2 l^3 / \left(3d^2\right)$ is a normalized factor. The relationship between depth and drag in the $x_1 -$ direction is

$$D_x = -\int_{-1}^{1} \mu \frac{\partial u}{\partial z}\Big|_{z=d} dx = -\frac{2\mu U l}{d} \psi_1^{/}(1). \tag{17}$$

Similarly $2\mu U l / d$ is normalized factor of drag in the $x -$ direction, which is $-\psi_1^{/}(1)$ and for $x_2 -$ direction, $-\psi_2^{/}(1)$ is a normalized drag:

$$D_y = -\int_{-1}^{1} \mu \frac{\partial v}{\partial z}\Big|_{z=d} dx = -\frac{2\mu V l}{d} \psi_2^{/}(1). \tag{18}$$

3 Integral transform method

Let us assume the general nonlinear second-order differential equation

$$\psi^{//}(\eta) = f\left(\eta, \psi(\eta), \psi^{/}(\eta)\right) \tag{19}$$

with corresponding boundary conditions

$$\begin{aligned} &\eta = \alpha_0 : \psi(\alpha_0) = \alpha \\ &\eta = \beta_0 : \psi(\beta_0) = \beta \end{aligned} \tag{20}$$

Integrating Eq. (19) with respect to η from α_0 to η twice yields

$$\psi(\eta) = \psi(\alpha_0) + (\eta - \alpha_0)\psi^{/}(\alpha_0) + \int_{\alpha_0}^{\eta} (\eta - \zeta) f\left(t, \psi(\zeta), \psi^{/}(\eta)\right) d\zeta \tag{21}$$

$$\psi(\eta) = \alpha + (\eta - \alpha_0)\psi^{/}(\alpha_0) + \int_{\alpha_0}^{\eta} (\eta - \zeta) f\left(\zeta, \psi(\zeta), \psi^{/}(\zeta)\right) d\zeta \tag{22}$$

By using the second boundary condition we can evaluate $\psi^{/}(\alpha_0)$ which is

$$\psi(\beta_0) = \beta = \alpha + (\beta_0 - \alpha_0)\psi^{/}(\alpha_0) + \int_{\alpha_0}^{\beta_0} (\beta_0 - \zeta) f\left(\zeta, \psi(\zeta), \psi^{/}(\zeta)\right) d\zeta \tag{23}$$

$$\frac{(\beta-\alpha)}{(\beta_0-\alpha_0)}-\frac{1}{(\beta_0-\alpha_0)}\int_{\alpha_0}^{\beta_0}(\beta_0-\zeta)\,f\left(\zeta,\psi(\zeta),\psi'(\zeta)\right)d\zeta=\psi'(\alpha_0) \tag{24}$$

Substituting Eqs. (24) into (22) results as

$$\psi(\eta)=\alpha+(\eta-\alpha_0)\left[\frac{(\beta-\alpha)}{(\beta_0-\alpha_0)}-\frac{1}{(\beta_0-\alpha_0)}\int_{\alpha_0}^{\beta_0}(\beta_0-\zeta)\,f(t,\psi(\zeta))dt\right]+\int_{\alpha_0}^{\eta}(\eta-\zeta)\,f\left(\zeta,\psi(\zeta),\psi'(\zeta)\right)d\zeta \tag{25}$$

$$\begin{aligned}
&\psi(\eta)=\psi_0(\eta)-\int_{\alpha_0}^{\beta_0}K(\eta,\zeta)\,f\left(\zeta,\psi(\zeta),\psi'(\zeta)\right)d\zeta\\
&\psi_0(\eta)=\alpha+\frac{(\eta-\alpha_0)(\beta-\alpha)}{(\beta_0-\alpha_0)}\\
&K(\eta,\zeta)=\frac{(\eta-\zeta)(\beta_0-\alpha_0)-(\eta-\alpha_0)(\beta_0-\zeta)}{(\beta_0-\alpha_0)},\quad \alpha_0<\zeta<\eta\\
&\qquad=\frac{(\eta-\alpha_0)(\beta_0-\zeta)}{(\beta_0-\alpha_0)}\qquad\qquad ,\quad \eta<\zeta<\beta_0
\end{aligned} \tag{26}$$

4 ITM solution for the long porous slider

Eq. (26) is the standard form of Variation Iteration Method-II [El-Sayed and El-Mongy (2018); Wazwaz and Kaur (2019); Faraz and Khan (2012)]. After applying the aforesaid method, Eqs. (7) to (9) can be expressed as follows:

$$\begin{aligned}
&\psi_3(\eta)=\frac{-2\eta^3(1+\beta_1+\beta_2)+3\eta(1+2\beta_2)(\eta+2\beta_1)}{\mathrm{A}_{11}}+\int_0^1 K(\eta,\zeta)\left[R\left(\psi_3'\psi_3''-\psi_3\psi_3'''\right)\right]d\zeta\\
&K(\eta,\zeta)=(1-\zeta)^3\left[\frac{\eta^3}{3!}\mathrm{C}_{11}-\frac{\eta^2(1+2\beta_2)}{2\mathrm{A}_{11}}-\frac{2\eta\beta_1(1+2\beta_2)}{\mathrm{A}_{11}}\right]+(1-\zeta)^2\left[-\frac{\eta^3}{3!}\mathrm{C}_{13}+\frac{\eta^2}{2\mathrm{A}_{11}}+\frac{\eta\beta_1}{\mathrm{A}_{11}}\right]\\
&\qquad+(1-\zeta)\left[-\frac{\eta^3}{3!}\mathrm{C}_{12}+\frac{\eta^2\beta_2}{\mathrm{A}_{11}}+\frac{2\eta\beta_2\beta_1}{\mathrm{A}_{11}}\right]+\frac{(\eta-\zeta)^3}{3!},\quad 0<\zeta<\eta\\
&\qquad=(1-\zeta)^3\left[\frac{\eta^3}{3!}\mathrm{C}_{11}-\frac{\eta^2(1+2\beta_2)}{2\mathrm{A}_{11}}-\frac{2\eta\beta_1(1+2\beta_2)}{\mathrm{A}_{11}}\right]+(1-\zeta)^2\left[-\frac{\eta^3}{3!}\mathrm{C}_{13}+\frac{\eta^2}{2\mathrm{A}_{11}}+\frac{\eta\beta_1}{\mathrm{A}_{11}}\right]\\
&\qquad+(1-\zeta)\left[-\frac{\eta^3}{3!}\mathrm{C}_{12}+\frac{\eta^2\beta_2}{\mathrm{A}_{11}}+\frac{2\eta\beta_2\beta_1}{\mathrm{A}_{11}}\right]\qquad\qquad ,\quad \eta<\zeta<1
\end{aligned} \tag{27}$$

where

$$\mathrm{C}_{11}=\frac{3(1+2\beta_2)(1+2\beta_1)}{\mathrm{A}_{11}}-1,\mathrm{C}_{12}=\frac{2\beta_2(3+6\beta_1)}{\mathrm{A}_{11}},\mathrm{C}_{13}=\frac{(3+6\beta_1)}{\mathrm{A}_{11}},\mathrm{A}_{11}=1+4(\beta_1+\beta_2)+12\beta_1\beta_2 \tag{28}$$

$$\psi_1(\eta)=\frac{1-\eta+\beta_2}{1+\beta_1+\beta_2}+\int_0^1 K(\eta,\zeta)R\left[\psi_1\psi_3'-\psi_3\psi_1'\right]d\zeta$$

$$K(\eta,\zeta)=\frac{\beta_1(1-\zeta+\beta_2)}{1+\beta_1+\beta_2}+\frac{\eta(1-\zeta+\beta_2)}{1+\beta_1+\beta_2}-(\eta-\zeta),\quad 0<\zeta<\eta \tag{29}$$

$$=\frac{\beta_1(1-\zeta+\beta_2)}{1+\beta_1+\beta_2}+\frac{\eta(1-\zeta+\beta_2)}{1+\beta_1+\beta_2},\quad \eta<\zeta<1$$

$$\psi_2(\eta)=\frac{1-\eta+\beta_2}{1+\beta_1+\beta_2}-\int_0^1 K(\eta,\zeta)R\left[\psi_3\psi_2'\right]d\zeta$$

$$K(\eta,\zeta)=\frac{\beta_1(1-\zeta+\beta_2)}{1+\beta_1+\beta_2}+\frac{\eta(1-\zeta+\beta_2)}{1+\beta_1+\beta_2}-(\eta-\zeta),\quad 0<\zeta<\eta \tag{30}$$

$$=\frac{\beta_1(1-\zeta+\beta_2)}{1+\beta_1+\beta_2}+\frac{\eta(1-\zeta+\beta_2)}{1+\beta_1+\beta_2},\quad \eta<\zeta<1$$

Furthermore, we can write Eqs. (27) to (30) in an iteration form as follows

$$\psi_{3,n+1}=\psi_{3,0}+\int_0^1 K(\eta,\zeta)\left[R\left(\psi_{3,n}'\psi_{3,n}''-\psi_{3,n}\psi_{3,n}'''\right)\right]d\zeta$$

where

$$\psi_{3,0}=\frac{-2\eta^3(1+\beta_1+\beta_2)+3\eta(1+2\beta_2)(\eta+2\beta_1)}{\mathrm{A}_{11}}$$

$$K(\eta,\zeta)=(1-\zeta)^3\left[\frac{\eta^3}{3!}\mathrm{C}_{11}-\frac{\eta^2(1+2\beta_2)}{2\mathrm{A}_{11}}-\frac{2\eta\beta_1(1+2\beta_2)}{\mathrm{A}_{11}}\right]+(1-\zeta)^2\left[-\frac{\eta^3}{3!}\mathrm{C}_{13}+\frac{\eta^2}{2\mathrm{A}_{11}}+\frac{\eta\beta_1}{\mathrm{A}_{11}}\right] \tag{31}$$

$$+(1-\zeta)\left[-\frac{\eta^3}{3!}\mathrm{C}_{12}+\frac{\eta^2\beta_2}{\mathrm{A}_{11}}+\frac{2\eta\beta_2\beta_1}{\mathrm{A}_{11}}\right]+\frac{(\eta-\zeta)^3}{3!},\quad 0<\zeta<\eta$$

$$=(1-\zeta)^3\left[\frac{\eta^3}{3!}\mathrm{C}_{11}-\frac{\eta^2(1+2\beta_2)}{2\mathrm{A}_{11}}-\frac{2\eta\beta_1(1+2\beta_2)}{\mathrm{A}_{11}}\right]+(1-\zeta)^2\left[-\frac{\eta^3}{3!}\mathrm{C}_{13}+\frac{\eta^2}{2\mathrm{A}_{11}}+\frac{\eta\beta_1}{\mathrm{A}_{11}}\right]$$

$$+(1-\zeta)\left[-\frac{\eta^3}{3!}\mathrm{C}_{12}+\frac{\eta^2\beta_2}{\mathrm{A}_{11}}+\frac{2\eta\beta_2\beta_1}{\mathrm{A}_{11}}\right]\qquad,\quad \eta<\zeta<1$$

$$\psi_{1,n+1} = \psi_{1,0} + \int_0^1 K(\eta,\zeta)\left[\psi_{1,n}\psi'_{3,n} - \psi_{3,n}\psi'_{1,n}\right]d\zeta$$

where

$$\psi_{1,0} = \frac{1-\eta+\beta_2}{1+\beta_1+\beta_2}$$

$$K(\eta,\zeta) = \frac{\beta_1(1-\zeta+\beta_2)}{1+\beta_1+\beta_2} + \frac{\eta(1-\zeta+\beta_2)}{1+\beta_1+\beta_2} - (\eta-\zeta), \quad 0<\zeta<\eta$$

$$= \frac{\beta_1(1-\zeta+\beta_2)}{1+\beta_1+\beta_2} + \frac{\eta(1-\zeta+\beta_2)}{1+\beta_1+\beta_2}, \quad \eta<\zeta<1 \tag{32}$$

$$\psi_{2,n+1} = \psi_{2,0} - \int_0^1 K(\eta,\zeta)\left[\psi_{3,n}\psi'_{2,n}\right]d\zeta$$

where

$$\psi_{2,0} = \frac{1-\eta+\beta_2}{1+\beta_1+\beta_2}$$

$$K(\eta,\zeta) = \frac{\beta_1(1-\zeta+\beta_2)}{1+\beta_1+\beta_2} + \frac{\eta(1-\zeta+\beta_2)}{1+\beta_1+\beta_2} - (\eta-\zeta), \quad 0<\zeta<\eta$$

$$= \frac{\beta_1(1-\zeta+\beta_2)}{1+\beta_1+\beta_2} + \frac{\eta(1-\zeta+\beta_2)}{1+\beta_1+\beta_2}, \quad \eta<\zeta<1 \tag{33}$$

5 Circular porous slider

From Fig. 1(b), we can see the circular slider, where L the radius of the slider which we assume comparatively is bigger than the width. Since slider is levitated so we fix our axes on the slider such that the ground is moving with a velocity component in x − direction. For the circular slider, we use the following similarity transform [Patel and Meher (2016)].

$$u = U\psi_5(\eta) + \frac{W}{d}x\,\psi'_4(\eta), v = \frac{W}{d}y\psi'_4(\eta), w = -2W\psi_4(\eta). \tag{34}$$

with the help of Eq. (34), Eqs. (2)-(4) takes the following form

$$\psi_4^{iv} - 2R\psi_4\psi_4''' - M^2\psi'_4 = 0 \tag{35}$$

$$\psi'_5 - R\left(\psi_5\psi'_4 - 2\psi_4\psi'_5\right) - M^2\psi_5 = 0 \tag{36}$$

$$-\frac{p}{\rho} = \frac{W^2\Lambda(x_1^2+x_2^2)}{2d} + \frac{1}{2}x_3^2 - \gamma x_{3,x_3} + C \tag{37}$$

in which Λ, C are constants and

$$\Lambda = \left(\psi_4^{/}(0)\right)^2 - \frac{1}{R}\psi_4^{///}(0). \tag{38}$$

the boundary condition is that on $x_3 = 0 \,\&\, d$:

$$\begin{aligned}
&\psi_4^{/}(0) = \beta_1\psi_4^{//}(0) =, \psi_4(0) = 0,\\
&\psi_4(1) = 1/2, \psi_4^{/}(1) = -\beta_2\psi_4^{//}(1),\\
&\psi_5(1) = -\beta_2\psi_5^{/}(1), \psi_5(0) - 1 = \beta_1\psi_5^{/}(0).
\end{aligned} \tag{39}$$

To normalize the lift, integrate over the bottom of the slider, as a result, we get the normalized factor $\pi\rho W^2 l^4 / 4d$

$$L = \frac{4d}{\pi\rho W^2 l^4}\iint_s (p - p_0)\, ds = \frac{1}{R^3}\Lambda. \tag{40}$$

The relationship between depth and drag in the x_1 -direction is

$$D_x = \frac{d}{\pi\mu U l^2}\iint_s H_{z,x} ds = -\frac{1}{R^3}\psi_5^{/}(1). \tag{41}$$

6 ITM solution for the circular slider

After applying the aforesaid method, Eqs. (35), (36) and (39) can be expressed as follows:

$$\begin{aligned}
\psi_4(\eta) &= \frac{-2\eta^3(1+\beta_1+\beta_2) + 3\eta(1+2\beta_2)(\eta+2\beta_1)}{2\mathrm{A}_{11}} + \int_0^1 K(\eta,\zeta)\left[-2R\psi_4\psi_4^{///}\right]d\zeta\\
K(\eta,\zeta) &= (1-\zeta)^3\left[\frac{\eta^3}{3!}\mathrm{C}_{11} - \frac{\eta^2(1+2\beta_2)}{2\mathrm{A}_{11}} - \frac{2\eta\beta_1(1+2\beta_2)}{\mathrm{A}_{11}}\right] + (1-\zeta)^2\left[-\frac{\eta^3}{3!}\mathrm{C}_{13} + \frac{\eta^2}{2\mathrm{A}_{11}} + \frac{\eta\beta_1}{\mathrm{A}_{11}}\right]\\
&\quad + (1-\zeta)\left[-\frac{\eta^3}{3!}\mathrm{C}_{12} + \frac{\eta^2\beta_2}{\mathrm{A}_{11}} + \frac{2\eta\beta_2\beta_1}{\mathrm{A}_{11}}\right] + \frac{(\eta-\zeta)^3}{3!}, \quad 0 < \zeta < \eta\\
&= (1-\zeta)^3\left[\frac{\eta^3}{3!}\mathrm{C}_{11} - \frac{\eta^2(1+2\beta_2)}{2\mathrm{A}_{11}} - \frac{2\eta\beta_1(1+2\beta_2)}{\mathrm{A}_{11}}\right] + (1-\zeta)^2\left[-\frac{\eta^3}{3!}\mathrm{C}_{13} + \frac{\eta^2}{2\mathrm{A}_{11}} + \frac{\eta\beta_1}{\mathrm{A}_{11}}\right]\\
&\quad + (1-\zeta)\left[-\frac{\eta^3}{3!}\mathrm{C}_{12} + \frac{\eta^2\beta_2}{\mathrm{A}_{11}} + \frac{2\eta\beta_2\beta_1}{\mathrm{A}_{11}}\right], \quad \eta < \zeta < 1
\end{aligned} \tag{42}$$

where

$$\mathrm{C}_{11} = \frac{3(1+2\beta_2)(1+2\beta_1)}{\mathrm{A}_{11}} - 1, \mathrm{C}_{12} = \frac{2\beta_2(3+6\beta_1)}{\mathrm{A}_{11}}, \mathrm{C}_{13} = \frac{(3+6\beta_1)}{\mathrm{A}_{11}}, \mathrm{A}_{11} = 1 + 4(\beta_1+\beta_2) + 12\beta_1\beta_2 \tag{43}$$

$$\psi_5(\eta)=\frac{1-\eta+\beta_2}{1+\beta_1+\beta_2}+\int_0^1 K(\eta,\zeta)R\left[\psi_4'\psi_5-2\psi_4\psi_5'\right]d\zeta$$

$$K(\eta,\zeta)=\frac{\beta_1(1-\zeta+\beta_2)}{1+\beta_1+\beta_2}+\frac{\eta(1-\zeta+\beta_2)}{1+\beta_1+\beta_2}-(\eta-\zeta),\quad 0<\zeta<\eta \tag{44}$$

$$=\frac{\beta_1(1-\zeta+\beta_2)}{1+\beta_1+\beta_2}+\frac{\eta(1-\zeta+\beta_2)}{1+\beta_1+\beta_2},\quad \eta<\zeta<1$$

Furthermore, we can write Eqs. (42) and (44) in an iteration form as follows

$$\psi_{4,n+1}=\psi_{4,0}+\int_0^1 K(\eta,\zeta)\left[-2R\psi_{4,n}\psi_{4,n}'''\right]d\zeta \tag{45}$$

where

$$\psi_{4,0}=\frac{-2\eta^3(1+\beta_1+\beta_2)+3\eta(1+2\beta_2)(\eta+2\beta_1)}{2\mathrm{A}_{11}}$$

$$K(\eta,\zeta)=(1-\zeta)^3\left[\frac{\eta^3}{3!}\mathrm{C}_{11}-\frac{\eta^2(1+2\beta_2)}{2\mathrm{A}_{11}}-\frac{2\eta\beta_1(1+2\beta_2)}{\mathrm{A}_{11}}\right]+(1-\zeta)^2\left[-\frac{\eta^3}{3!}\mathrm{C}_{13}+\frac{\eta^2}{2\mathrm{A}_{11}}+\frac{\eta\beta_1}{\mathrm{A}_{11}}\right]$$

$$+(1-\zeta)\left[-\frac{\eta^3}{3!}\mathrm{C}_{12}+\frac{\eta^2\beta_2}{\mathrm{A}_{11}}+\frac{2\eta\beta_2\beta_1}{\mathrm{A}_{11}}\right]+\frac{(\eta-\zeta)^3}{3!},\quad 0<\zeta<\eta$$

$$=(1-\zeta)^3\left[\frac{\eta^3}{3!}\mathrm{C}_{11}-\frac{\eta^2(1+2\beta_2)}{2\mathrm{A}_{11}}-\frac{2\eta\beta_1(1+2\beta_2)}{\mathrm{A}_{11}}\right]+(1-\zeta)^2\left[-\frac{\eta^3}{3!}\mathrm{C}_{13}+\frac{\eta^2}{2\mathrm{A}_{11}}+\frac{\eta\beta_1}{\mathrm{A}_{11}}\right]$$

$$+(1-\zeta)\left[-\frac{\eta^3}{3!}\mathrm{C}_{12}+\frac{\eta^2\beta_2}{\mathrm{A}_{11}}+\frac{2\eta\beta_2\beta_1}{\mathrm{A}_{11}}\right],\quad \eta<\zeta<1$$

$$\psi_{5,n+1}=f_0+\int_0^1 K(\eta,\zeta)\left[\psi_{5,n}\psi_{4,n}'-2\psi_{4,n}\psi_{5,n}'\right]d\zeta$$

where

$$\psi_{5,0}=\frac{1-\eta+\beta_2}{1+\beta_1+\beta_2} \tag{46}$$

$$K(\eta,\zeta)=\frac{\beta_1(1-\zeta+\beta_2)}{1+\beta_1+\beta_2}+\frac{\eta(1-\zeta+\beta_2)}{1+\beta_1+\beta_2}-(\eta-\zeta),\quad 0<\zeta<\eta$$

$$=\frac{\beta_1(1-\zeta+\beta_2)}{1+\beta_1+\beta_2}+\frac{\eta(1-\zeta+\beta_2)}{1+\beta_1+\beta_2},\quad \eta<\zeta<1$$

One can use any software to solve Eqs. (40) and (41) by using ITM. In our study, we have used MATHEMATICA.

7 Results and discussion

ITM has been applied to compute the solution of the problems given in Eqs. (7)-(9), (12), (35), (36), and (39). Obtained solutions have been presented in the form of tables and graphs. Tabs. 1 and 2 display the effects of the slip on the dynamic properties of a slider.

Table 1: Properties of the long porous slider. Normalized lift Λ, normalized x_1- direction drag, and normalized x_2- direction drag

		Present				[10]			
β_1, β_2	M^2	R	Λ	$-\psi_1'(1)$	$-\psi_2'(1)$	R	Λ	$-\psi_1'(1)$	$-\psi_2'(1)$
0, 0	0	0.2	62.334	0.8962	0.9322	0.2	62.33	0.896	0.932
-	-	0.5	26.341	0.7601	0.8364	0.5	26.34	0.760	0.836
-	-	2.0	8.4123	0.3348	0.4675	2.0	8.412	0.334	0.467
-	-	5.0	4.9172	0.0632	0.1238	5.0	4.917	0.063	0.123
-	-	20	3.2678	0	0	20	3.267	0	0
-	-	50	2.9092	0	0	50	2.909	0	0
0.1, 0.1	2	0.2	39.27	0.743	0.780	/	/	/	/
-	4	0.5	16.78	0.626	0.704	/	/	/	/
-	6	2.0	6.596	0.4372	0.2536	/	/	/	/
-	10	5.0	3.436	0.3245	0	/	/	/	/
	20	20.0	2.440	0.1520	0	/	/	/	/
	50	50.0	2.240	0	0	/	/	/	/
0.1, 1	2	0.2	20.31	0.424	0.463	/	/	/	/
-	4	0.5	8.859	0.357	0.436	/	/	/	/
-	6	2.0	3.159	0.160	0.321	/	/	/	/
-	10	5.0	2.050	0.035	0.123	/	/	/	/
	20	20.0	1.513	0	0.0632	/	/	/	/
	50	50.0	1.391	0	0.012	/	/	/	/
0.1, 10	2	0.2	5.316	0.064	0.082	/	/	/	/
-	4	0.5	2.702	0.046	0.080	/	/	/	/
-	6	2.0	1.413	0.013	0	/	/	/	/
-	10	5.0	1.175	0.002	0	/	/	/	/
	20	20.0	1.068	0	0	/	/	/	/
	50	50.0	1.047	0	0	/	/	/	/
1, 1	2	0.2	9.727	0.275	0.315	/	/	/	/
-	4	0.5	4.591	0.210	0.288	/	/	/	/
-	6	2.0	2.048	0.068	0.172	/	/	/	/
	10	5.0	1.569	0.011	0.047	/	/	/	/
	20	20.0	1.355	0	0	/	/	/	/
	50	50.0	1.315	0	0	/	/	/	/

Table 2: Properties of the circular porous slider. Normalized lift Λ, normalized drag $-\psi_5'(1)$

			Present		[10]	
β_1, β_2	M^2	R	Λ	$-\psi_5'(1)$	Λ	$-\psi_5'(1)$
0, 0	0	0.2	30.783	0.9141	30.78	0.914
-	-	0.5	12.793	0.7978	12.79	0.797
-	-	2.0	3.8332	0.3923	3.833	0.392
-	-	5.0	2.0195	0.0852	2.019	0.085
-	-	20	1.3491	0	1.349	0
-	-	50	1.1945	0	1.194	0
0.1, 0.1	2	0.2	19.33	0.761	/	/
-	4	0.5	8.089	0.663	/	/
-	6	2.0	2.503	0.310	/	/
-	10	5.0	1.445	0.1014	/	/
	20	20.0	0.994	0	/	/
	50	50.0	0.908	0	/	/
0.1, 1	2	0.2	9.853	0.441	/	/
-	4	0.5	4.130	0.394	/	/
-	6	2.0	1.288	0.129	/	/
-	10	5.0	0.752	0.0145	/	/
	20	20.0	0.529	0	/	/
	50	50.0	0.483	0	/	/
0.1, 10	2	0.2	6.438	0.084	/	/
-	4	0.5	2.699	0.076	/	/
-	6	2.0	0.841	0.015	/	/
-	10	5.0	0.488	0	/	/
	20	20.0	0.338	0	/	/
	50	50.0	0.305	0	/	/
1, 1	2	0.2	4.611	0.294	/	/
-	4	0.5	2.043	0.244	/	/
-	6	2.0	0.776	0.0215	/	/
	10	5.0	0.549	0	/	/
	20	20.0	0.466	0	/	/
	50	50.0	0.453	0	/	/

It shows that normalized lift and drag goes down as the slip and/or Reynolds number goes up (see Tabs. 1 and 2). The lift (per area) of a strip slider is much greater than the circular slider, whenever the drag remains the same in both cases. The effect of slip could be substantial, dropping the drag much more than the lift.

Furthermore, the effects of the transverse magnetic field and Reynolds number on typical velocity profile are displayed in Figs. 2 to 23 for the strip and circular slider. From Figs. 2 to 22, the effects of the transverse magnetic field and Reynolds number can be summed

up as follows. For small magnetic field and Reynolds number, the velocity profile is almost linear or parabolic. In case of the large magnetic field and Reynolds number, a boundary layer occurs near the ground.

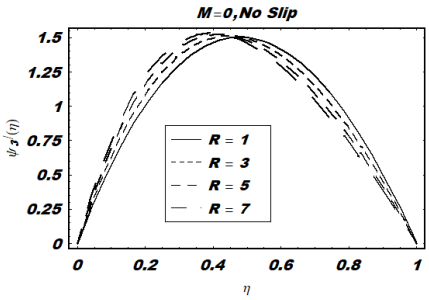

Figure 2: Similarity function $\psi_3^{/}$ for no-slip

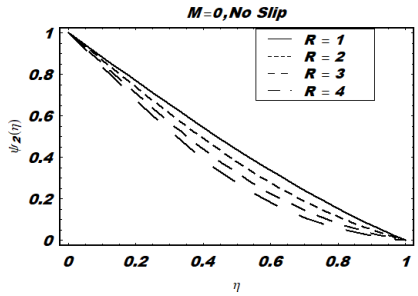

Figure 3: Similarity function ψ_2 for no-slip

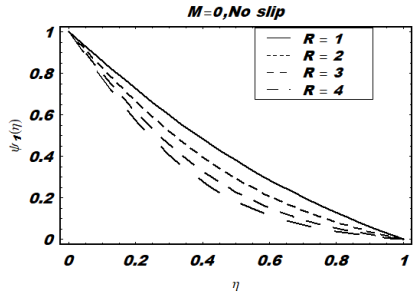

Figure 4: Similarity function ψ_1 for no-slip

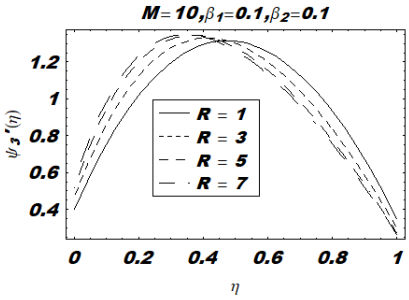

Figure 5: Similarity function $\psi_3^{/}$ with slip

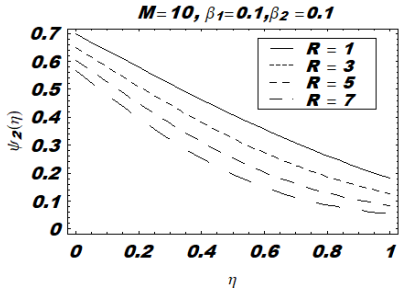

Figure 6: Similarity function ψ_2 with slip

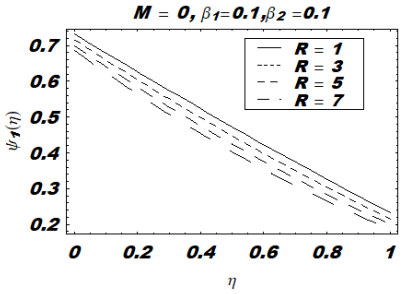

Figure 7: Similarity function ψ_1 with slip

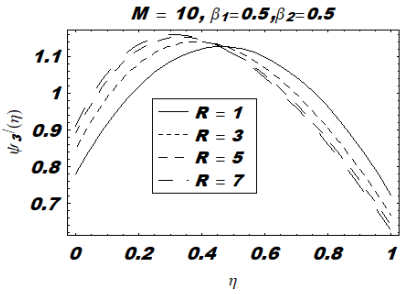

Figure 8: Similarity function $\psi_3^{/}$ with slip

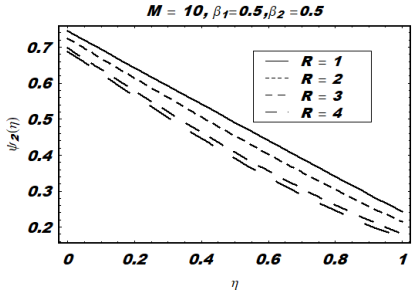

Figure 9: Similarity function ψ_2 with slip

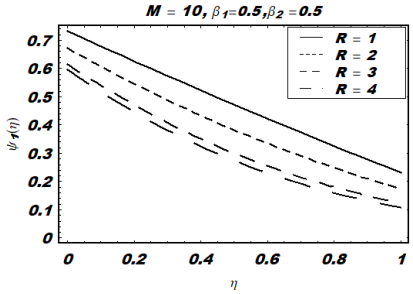

Figure 10: Similarity function ψ_1 with slip

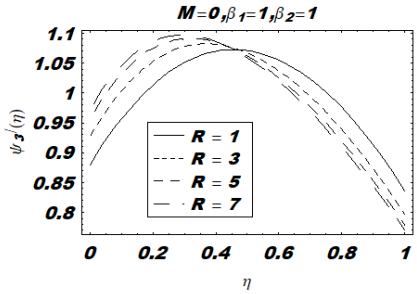

Figure 11: Similarity function $\psi_3^{/}$ with slip

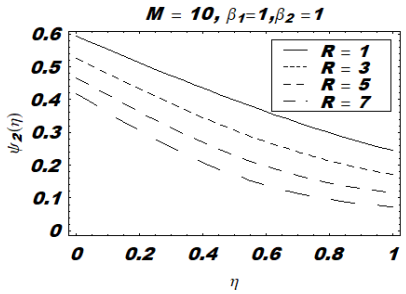

Figure 12: Similarity function ψ_1 with slip

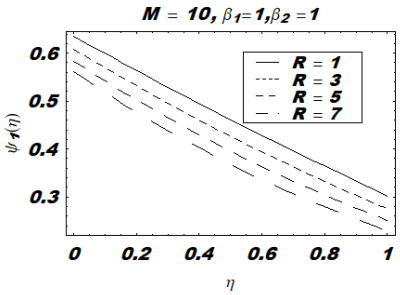

Figure 13: Similarity function $\psi_3^{/}$ with slip

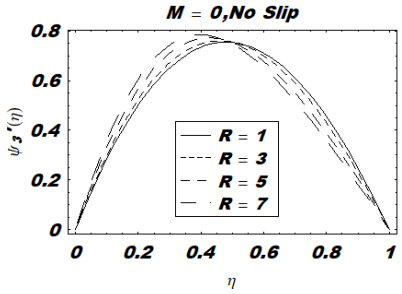

Figure 14: Similarity function $\psi_4^{/}$ with no-slip

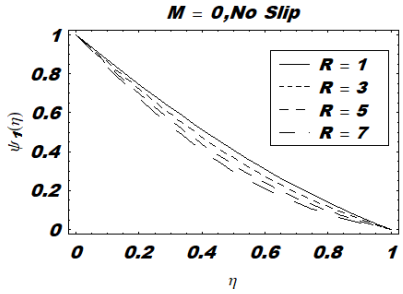

Figure 15: Similarity function ψ_5 with slip

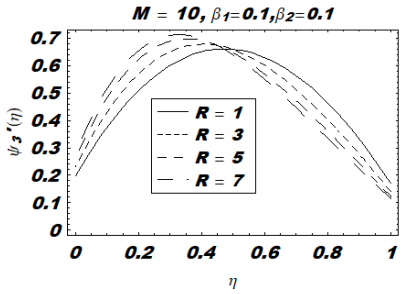

Figure 16: Similarity function $\psi_4^{/}$ with slip

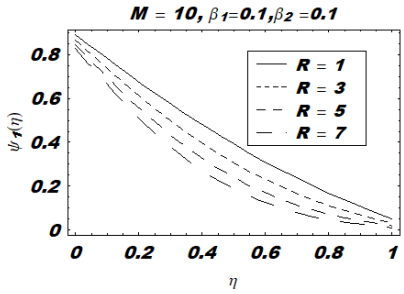

Figure 17: Similarity function ψ_5 with slip

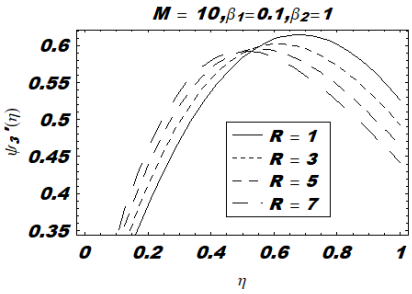

Figure 18: Similarity function $\psi_4^{/}$ with slip

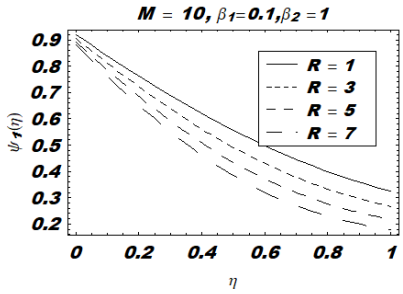

Figure 19: Similarity function ψ_5 with slip

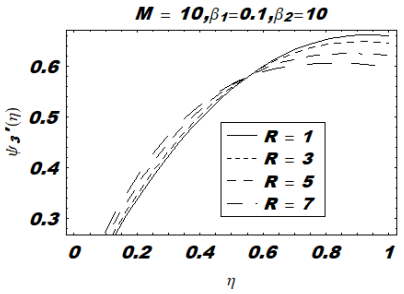

Figure 20: Similarity function ψ_4' with slip

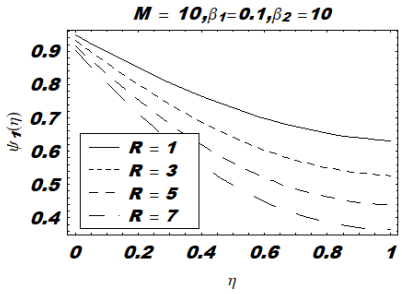

Figure 21: Similarity function ψ_5 with slip

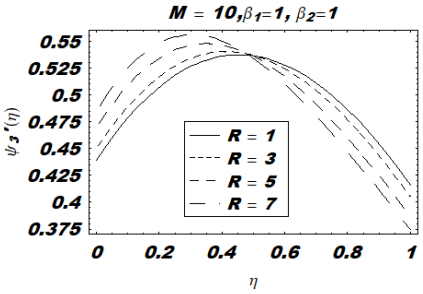

Figure 22: Similarity function ψ_4' with slip

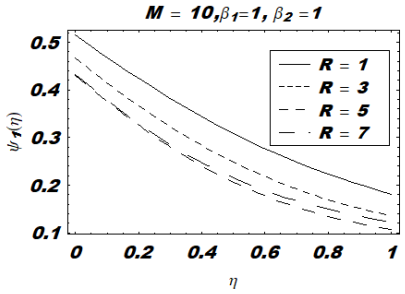

Figure 23: Similarity function ψ_5 with slip

For strip slider, the effect of Reynolds number, in case of slip and the magnetic field is shown in Figs. 5 to 13. It is observed that the velocity profile is very much changed. Figs. 6, 7, 9 and 10, 12 and 13 display that slips near the ground reduce the lateral velocity much more than slip on the slider. Moreover, increasing the magnetic parameter decreases the lateral velocity components further. Similarly, the effects of Reynolds number on typical velocity distribution is displayed in Figs. 14 to 23 for the circular slider. The behaviour of velocity profiles is similar for stipe and circular slider in case of no-slip (see Figs. 2, 3, 14 & 15). Also, velocity profiles are behaving in a similar fashion as stipe slider i.e., parabolic or linear for low Reynolds number and for large Reynolds number boundary layer formed near the surface. Figs. 16 to 23 determine the effect of the slip parameter on the velocity components corresponding to different values of the Reynolds number. These pictorial descriptions demonstrate that velocity profiles decrease with an increase in slip parameters and this decrease become even further after applying the magnetic field. This is due to the fact that slip hinders the fluid particles and displays the motion in the vicinity.

These results qualitatively agree with expectation since the application of a transverse magnetic field normal to the lateral flow directions has a tendency to create a drag-like Lorentz force. This force decreases the lateral velocity components. Lift and drag components are important physical quantities for a porous slider. It is interesting to note that the lift is free of translation, but the drag components and depend on the crossflow.

The effectiveness of a porous slider can be enhanced by making the ratio of friction force to lift smaller. As pointed out by Khan et al. [Khan, Faraz, Yildirim et al. (2011)], porous slider should be operated at cross-flow Reynolds number less than unity for optimum efficiency. Tab. 1 shows that the fact that porous sliders should be operated at small values of still remains valid even when an external uniform magnetic field is applied. Moreover, from the optimum efficiency point of view, it is more efficient to move a flat slider on a fluid subject to a magnetic field with high intensity.

8 Conclusions

In this study, we have compiled different studies altogether. Different researchers have analyzed fluid flow on stripe slider, without slip and some were interested only in circular slider without slip. Wang presented the comparative study of both stripe and circular slider and added velocity slip but did not cover the effects of the magnetic field. We were concerned with a theoretical investigation of the steady three-dimensional flow of a viscous fluid between a porous slider and ground in the presence of a transverse uniform magnetic field with velocity slip. The effects of values physical parameter like Reynolds number and magnetic parameter on the lateral velocity profiles, lift and drag components were presented in graphical and tabular form in the presence of velocity slip. It is hoped that the results of the present study would be useful for the understanding of various technological problems related to porous sliders, where magnetic and velocity slip are the main physical parameters.

Conflicts of Interest: The authors declare that they have no conflicts of interest to report regarding the present study.

References

Awati, V. B.; Jyoti, M. (2016): Homotopy analysis method for the solution of lubrication of a long porous slider. *Applied Mathematics and Nonlinear Sciences*, vol. 1, no. 2, pp. 507-516.

El-Sayed, T. A.; El-Mongy, H. H. (2018): Application of variational iteration method to free vibration analysis of a tapered beam mounted on two-degree of freedom subsystems. *Applied Mathematical Modelling*, vol. 58, pp. 349-364.

Faraz, N. (2011): Study of the effects of the Reynolds number on circular porous slider via variational iteration algorithm-II. *Computers & Mathematics with Applications*, vol. 61, no. 8, pp. 1991-1994.

Faraz, N.; Khan, Y. (2012): Study of the dynamics of rotor-spun composite yarn spinning process in forced vibration. *Textile Research Journal*, vol. 82, no. 3, pp. 255-258.

Faraz, N.; Khan, Y.; Austin, F. (2010): An alternative approach to differential-difference equations using the variational iteration method. *Zeitschrift für Naturforschung A*, vol. 65, no. 12, pp. 1055-1059.

Faraz, N.; Khan, Y.; Lu, D. C.; Goodarzi, M. (2019): Integral transform method to solve the problem of porous slider without velocity slip. *Symmetry (Basel)*, vol. 11, no. 6, pp. 791.

Ghoreishi, M.; Ismail, A. I. B. M.; Rashid, A. (2012): The one step optimal homotopy analysis method to circular porous slider. *Mathematical Problems in Engineering*.

Khan, Y.; Faraz, N.; Yildirim, A.; Wu, Q. (2011): A series solution of the long porous slider. *Tribology Transactions*, vol. 54, no. 2, pp. 187-191.

Khan, Y.; Wu, Q.; Faraz, N.; Yildirim, A.; Mohyud-Dind, S. T. (2011): Three-dimensional flow arising in the long porous slider: an analytic solution. *Zeitschrift für Naturforschung A*, vol. 66, no. 8-9, pp. 507-511.

Madani, M.; Khan, Y.; Mahmodi, G.; Faraz, N.; Yildirim, A. et al. (2012). Application of homotopy perturbation and numerical methods to the circular porous slider. *International Journal of Numerical Methods for Heat & Fluid Flow*, vol. 22, no. 6, pp. 705-717.

Patel, H. S.; Meher, R. (2016): Analytical investigation of jeffery-hamel flow by modified Adomian decomposition method. *Ain Shams Engineering Journal*, vol. 9, no. 4, pp. 599-606.

Sinha, P.; Adamu, G. (2017): Analysis of thermal effects in a long porous rough slider bearing. *Proceedings of the National Academy of Sciences, India Section A: Physical Sciences*, vol. 87, no. 2, pp. 279-290.

Skalak, F.; Wang, C. Y. (1975): Fluid dynamics of a long porous slider. *Journal of Applied Mechanics*, vol. 42, no. 4, pp. 893-894.

Turkyilmazoglu, M. (2016): Magnetic field and slip effects on the flow and heat transfer of stagnation point Jeffrey fluid over deformable surfaces. *Zeitschrift für Naturforschung A*, vol. 71, no. 6, pp. 549-556.

Turkyilmazoglu, M. (2018): Analytical solutions to mixed convection MHD fluid flow induced by a nonlinearly deforming permeable surface. *Communications in Nonlinear Science and Numerical Simulation*, vol. 63, pp. 373-379.

Turkyilmazoglu, M. (2019a): Latidutinally deforming rotating sphere. *Applied Mathematical Modelling*, vol. 71, no. 2, pp. 1-11.

Turkyilmazoglu, M. (2019b): MHD natural convection in saturated porous media with heat generation/absorption and thermal radiation. *Archives of Mechanics*, vol. 71, no. 1, pp. 49-64.

Turkyilmazoglu, M. (2019c): Accelerating the convergence of Adomian decomposition method (ADM). *Journal of Computational Science*, vol. 31, pp. 54-59.

de Vargas Lisbôa, T.; Marczak, R. J. (2018): Adomian decomposition method applied to anisotropic thick plates in bending. *European Journal of Mechanics-A/Solids*, vol. 70, no. 3, pp. 95-114.

Wang, C. Y. (1974): Fluid dynamics of the circular porous slider. *Journal of Applied Mechanics*, vol. 41, no. 2, pp. 343-347.

Wang, C. Y. (1974): Erratum: "Fluid dynamics of the circular porous slider". *Journal of Applied Mechanics*, vol. 41, pp. 343-347.

Wang, C. Y. (1978): Erratum: "Fluid dynamics of the circular porous slider". *Journal of Applied Mechanics*, vol. 45, no. 1, pp. 236.

Wang, C. Y. (2012): A porous slider with velocity slip. *Fluid Dynamics Research*, vol. 44, no. 6, 065505.

Wazwaz, A. M.; Kaur, L. (2019): Optical solitons and Peregrine solitons for nonlinear Schrödinger equation by variational iteration method. *Optik*, vol. 179, pp. 804-809.